Qualitative theory of finite-particle quantum systems. Comparison of fully quantum, semi-quantum and completely classical models.

B. I. Zhilinskii

Université du Littoral Côte d'Opale, 59 140 Dunkerque, France

October 2016

Simposium on advances in semi-classical methods in mathematics and physics

Groningen, Nederland

Collaborators

Toshihiro Iwai - Kyoto University, Japan

Guillaume Dhont - ULCO Dunkerque, France

Dmitrii Sadovskii - ULCO Dunkerque, France

Frédéric Faure - Institut Fourier, Grenoble, France

Plan

1. What I mean by qualitative effects.

   Quantum bifurcations

   Reorganization of band structure

2. Quantum, semi-quantum, and classical models

   Simple molecular examples

   Energy-reflection symmetry

   Quaternionic models

   Real symmetric Hamiltonians

3. Solid state analogy.

   Topological phases of matter.

4. Mathematical correspondence.

   $\mathbb{R}, \mathbb{C}, \mathbb{H}$ trinity.

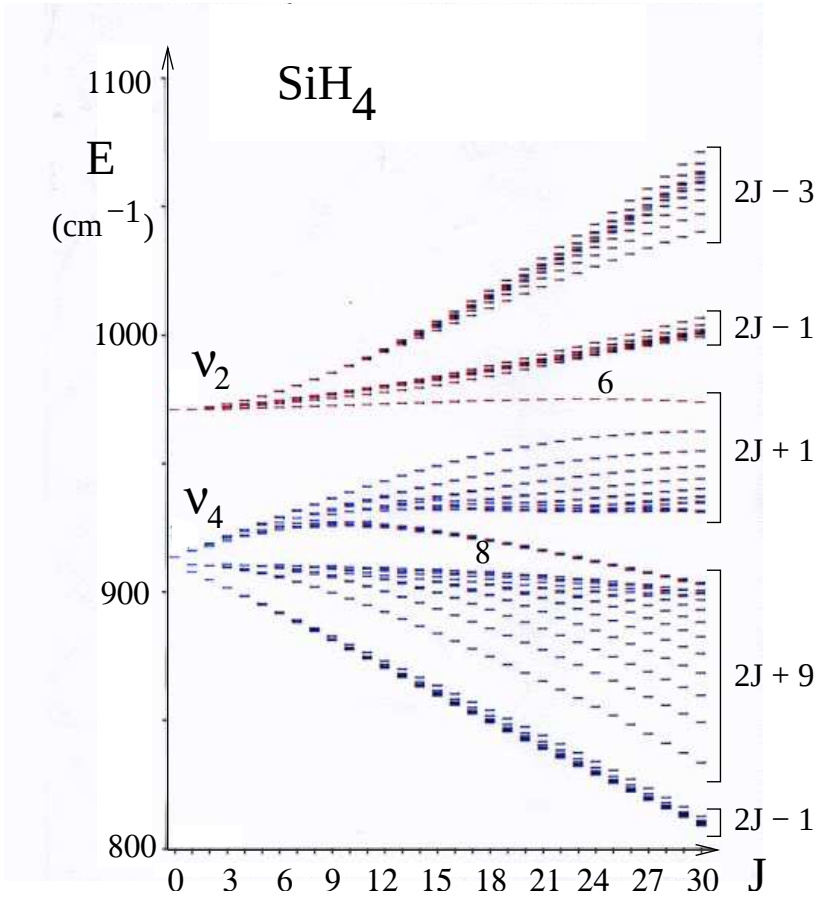

Reduced rovibrational energy as a function of rotational quantum number J for lowest vibrational bands ν_4 (F_2 symmetry type) and ν_2 (E symmetry type) of SiH_4 tetrahedral molecule (T_d point symmetry group).

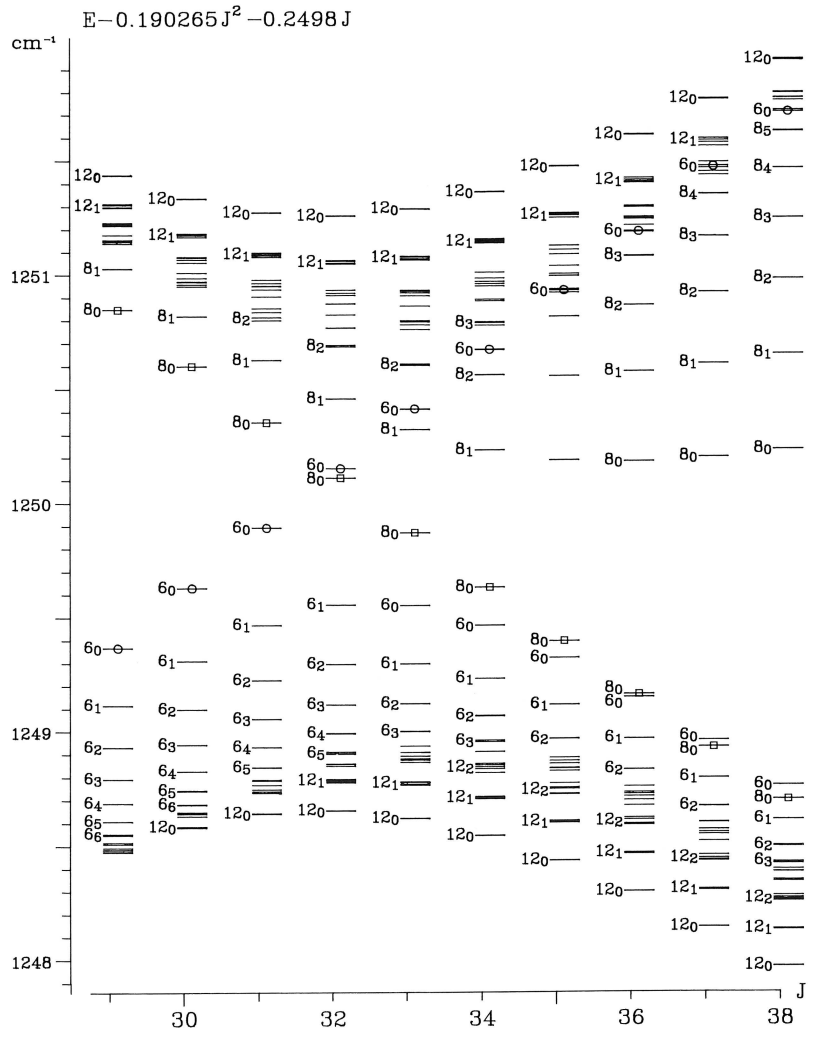

Upper branch of ν_3 and lower branch of $2\nu_4$ bands of CF_4 molecule with T_d point symmetry group of the equilibrium configuration.

Energy level representation in

Energy (E) - Angular momentum (J)

coordinates corrected with the scalar function $E(J)$ to see better the band structure and the evolution of internal structure of bands as a function of a strict integral of motion J.

Qualitative features to explain:

i) Rotational clusters (6-fold, 8-fold, 12-fold quasidegenerate)

ii) Modification of cluster structure (appearance of 12-fold cluster as J increases).

iii) Number of energy levels in a band:
$2J + 1 + \Delta$, ??? Δ ???

iv) Rules for redistribution of energy levels between bands.

Qualitative phenomena

Quantum bifurcations, cluster structure. [1]

Quantum monodromy and its generalizations. [2]

Energy bands and their rearrangements. [3]

[1] Ann. Phys. (N.Y.) **184**, 1-32 (1988); Phys. Rep. **341**, 85-171 (2001); In Meyers, Robert (Ed.) Encyclopedia of Complexity and Systems Science, Springer New York 2009, Part 17, Pages 7135-7154.

[2] Phys. Lett. A **256**, 235-44 (1999); Phys. Rev. Lett. **93**, 024302-1-4 (2004); Ann. Henri Poincare. **7**, 1099–1211 (2006); Ann.Phys. (N.Y) **322**, 164–200 (2007).

[3] Europhys. Lett. **6**, 573-78 (1988); Phys. Rev. Lett. **85**, 960-963 (2000); Phys. Lett. A **302**, 242-252 (2002); Ann. Phys. (N.Y) **326**, 3013-3066 (2011); Acta Appl. Math. **20**, 153-175 (2012); Phys. Lett. A **377** 2481-2486 (2013) ; Theoret. Chem. Accounts, **133**, 1501 (2014); Acta Appl. Math, **137**, 97-121 (2015).

General idea of qualitative approach

- To study a family of objects/models depending on a number of *control parameters* (external or internal).
- To find characteristics which are defined for almost all values of control parameters and are *piece-wise constant.*

This allows to split the space of control parameters into disjoint regions by a codimension one boundary (*wall*). Qualitative modifications under control parameter variation are associated with *wall-crossing.*

We use the notion "*wall-crossing*" just to show that for the studied molecular examples the qualitative description can be regarded as one concrete realization of general "wall-crossing" formalism[a].

[a] see M. Kontsevich, Y. Soibelman, Wall-crossing structures in Donaldson-Thomas invariants, integrable systems and Mirror Symmetry. LNM, in press; arXiv:1303.3253

D.Gaiotto, G.W. Moore, A. Neitzke, Wall-crossing, Hitchin systems, and the WKB approximation, Adv. Math. 234, 239-403 (2013)

Construction of semi-quantum model

"*Slow*" variables - classical.

"*Fast*" variables - quantum.

Classical phase space - *base* of the fiber bundle.

Hamiltonian - *matrix symbol* defined over classical phase space.

Eigenvectors of the Hamiltonians - *fibers* of vector bundle.

Topological invariants of eigenbundles - *Chern numbers, ...*

Dimension of matrix Hamiltonian - *number of bands* - rank of vector bundle.

Bands are *isolated* if there are *no degeneracy points* of eigenvalues.

Eigenline bundles are characterized by topological invariant - *Chern number.*

Degeneracy points are responcible for modification of the band structure and of the set of Chern numbers.

Symmetry should be taken into account

(spatial, dynamical, time-reversal, ...)

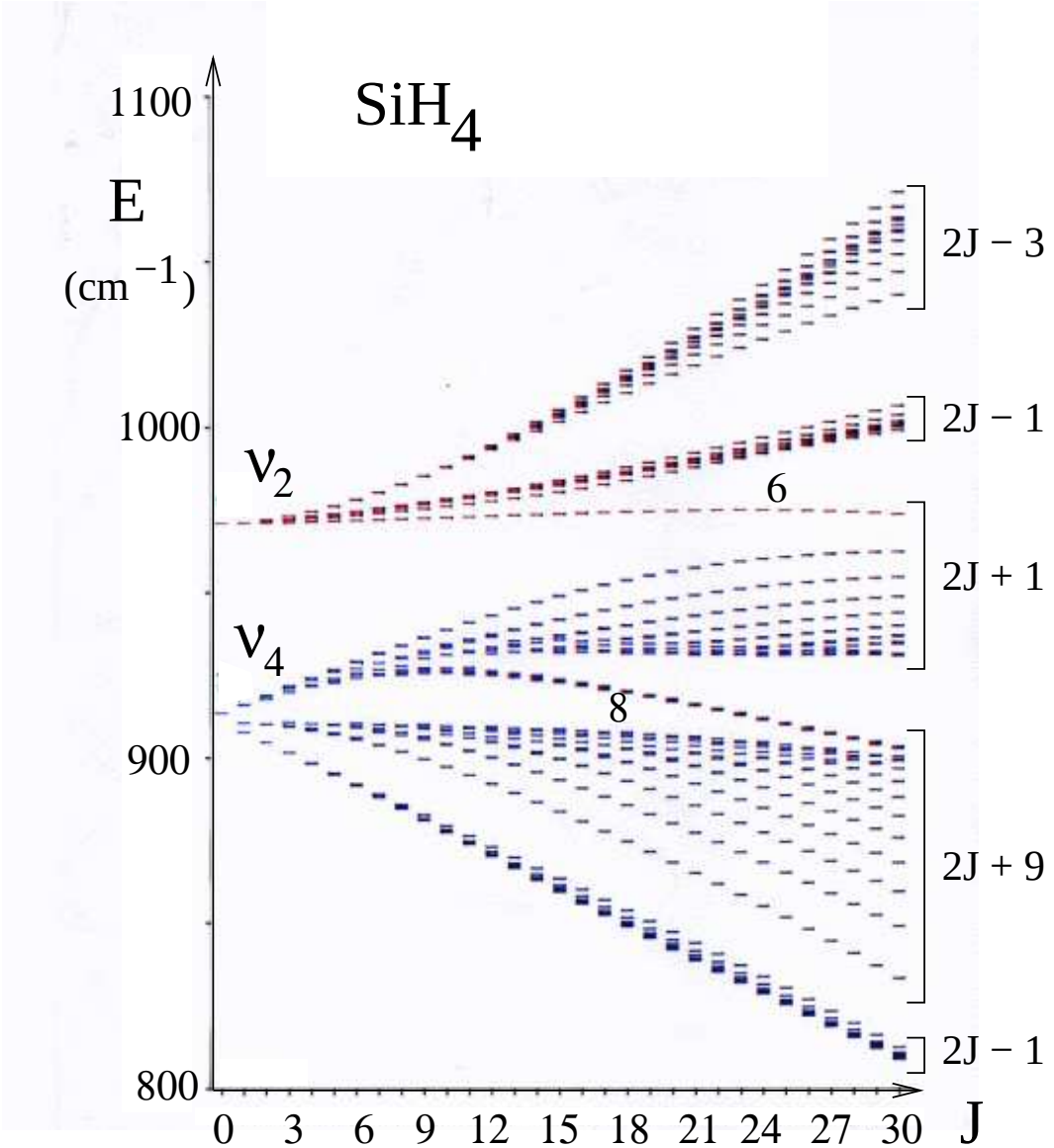
SiH4
1100
E
(cm−1)
1000
900
800
ν2
ν4
6
8
2J − 3
2J − 1
2J + 1
2J + 9
2J − 1
0 3 6 9 12 15 18 21 24 27 30
J

Energy bands and corresponding Chern numbers for SiH_4 molecular example.

Band	$J \sim 8$ Numb. lev.	$J \sim 8$ Chern numb.	$J \sim 30$ Numb. lev.	$J \sim 30$ Chern.numb.
ν_2 (upper)	$2J-3$	-4	$2J-3$	-4
ν_2 (lower)	$2J+5$	$+4$	$2J-1$	-2
ν_4 (upper)	$2J+3$	$+2$	$2J+1$	0
ν_4 (middle)	$2J+1$	0	$2J+9$	$+8$
ν_4 (lower)	$2J-1$	-2	$2J-1$	-2

Simplest molecular example of band rearrangement.

Spin-rotation coupling in presence of magnetic field.

$$H(t) = t\mathbf{N} \cdot \mathbf{S} + (1-t)S_z. \qquad (1)$$

Two limiting cases

i) $t \sim 0$: spin-rotation coupling is negligible; interaction of a spin with magnetic field is essential.

ii) $t \sim 1$: spin-rotation coupling is essential; interaction of a spin with magnetic field is negligible.

Although $H(t)$ is $SO(2)$ invariant, the phenomenon is **topological**.

Redistribution of quantum energy levels between energy bands along with variation of control parameter t. The model Hamiltonian is written for a fixed value of the angular momentum.

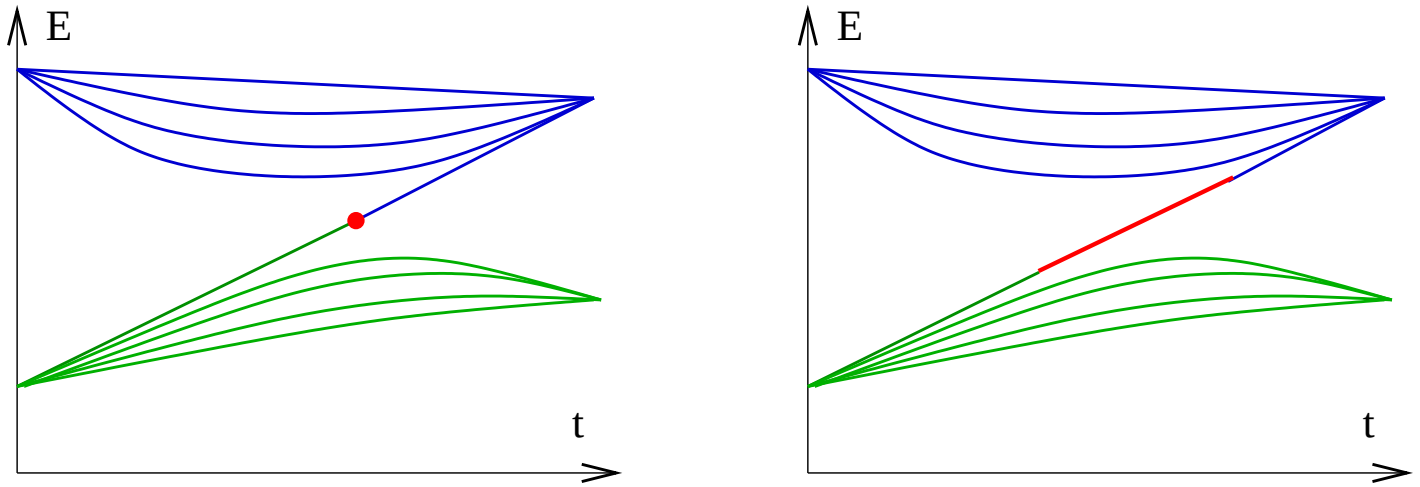

Two possible physical interpretations :

Left : Redistributing level - “edge state“ - is assigned to lower or to upper band for all control parameter values except for t_0 - “zero energy“ state (red point).

Right : Redistributing level changes its character from “regular“ to “edge“ and back to “regular “ states (red - “edge state“).

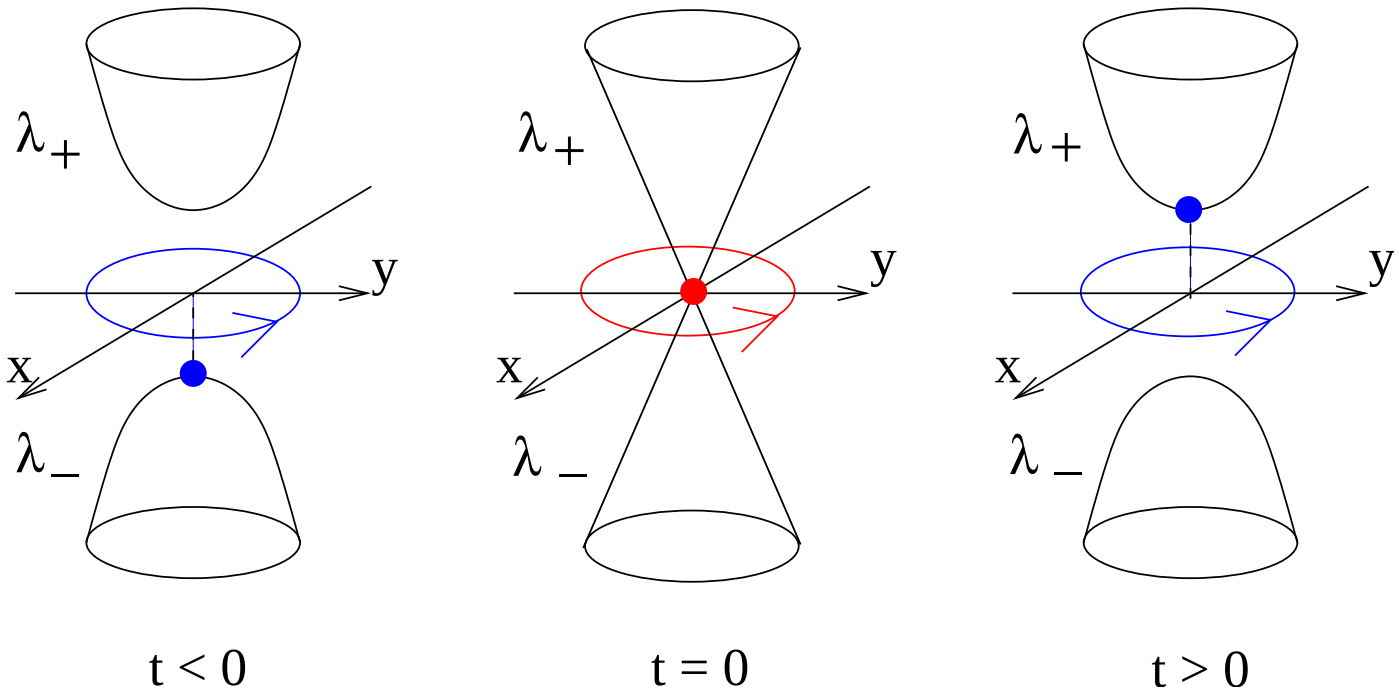

Schematic representation of the evolution of eigenvalues of a local linearized model Hamiltonian (of A symmetry class) in a two-level approximation along with variation of a control parameter t crossing the boundary of the iso-Chern domain. Exceptional points (blue points) in the chosen representation are shown.

T. Iwai, B. Zhilinskii, Qualitative features of the rearrangement of molecular energy spectra from a "wall-crossing" perspective. Phys. Lett. A 377 (2013) 2481-2486

Redistribution of quantum energy levels between energy bands in isolated molecules as a function of the integral of motion, N.

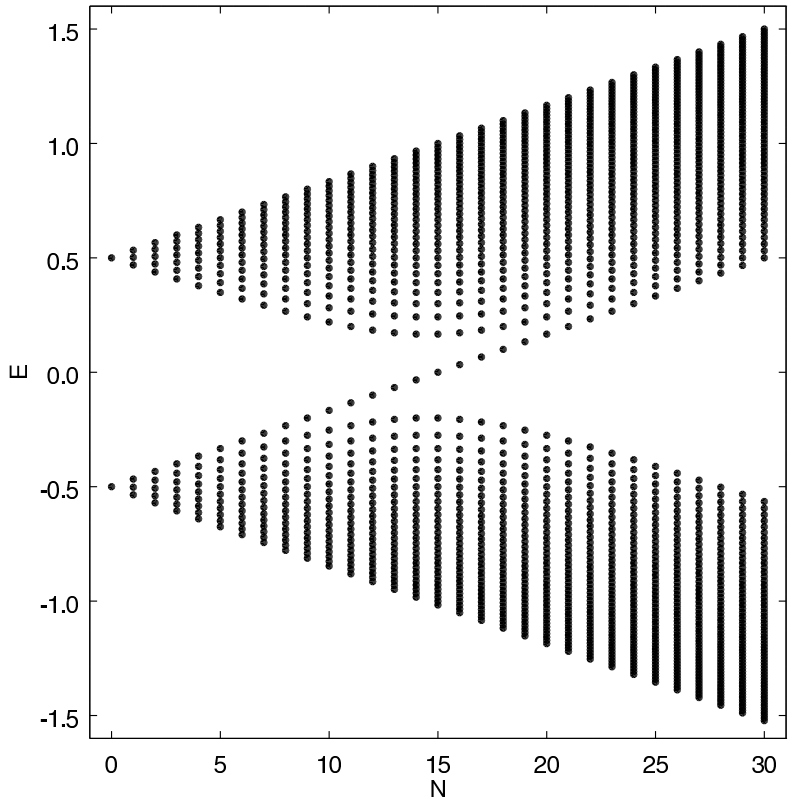

Quantum number N labels irreps of the dynamical symmetry group of the problem and takes discrete values. The total number of energy levels for two bands depends on N.

Schematic view of the joint spectrum of two commuting observables E, j and its evolution as a function of control parameter t.

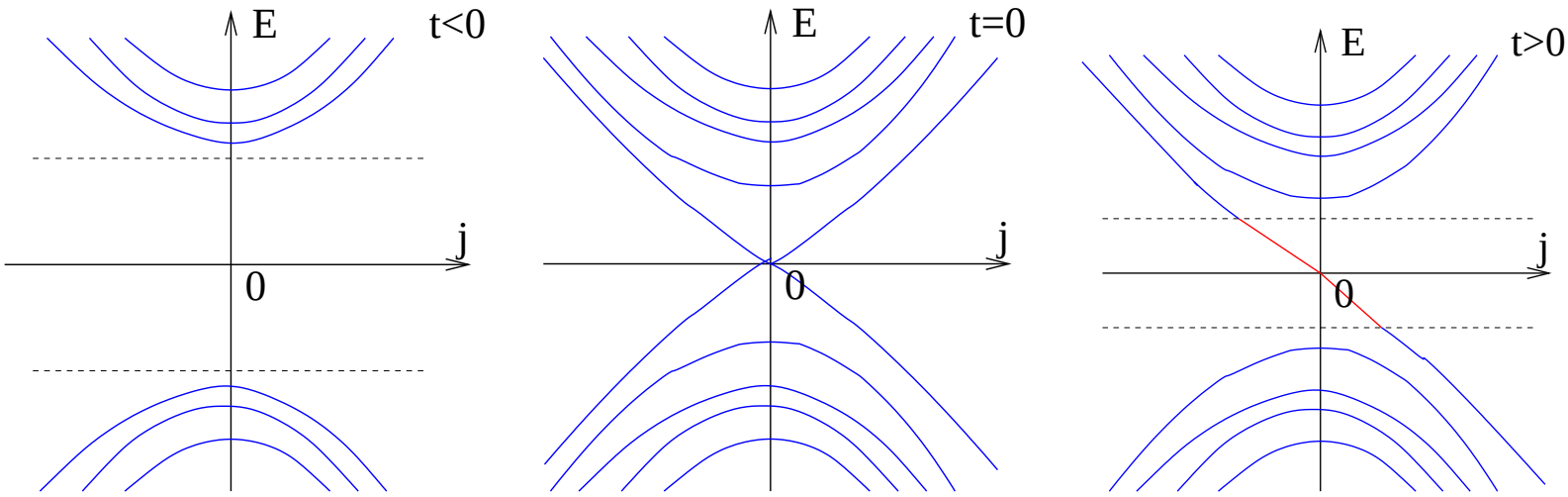

Two isolated energy bands (each has internal structure described by two quantum numbers) transform into two 2D-bands connected by 1D-isthmus.

New qualitative structure : " **isthmus***".*

Hamiltonian with energy-reflection symmetry (pseudo-symmetry)

$$H_{\rm quantum} = \begin{pmatrix} A + \delta L_z + dL_z^2 & \bar{\gamma} L_- \\ \gamma L_+ & -A - \delta L_z - dL_z^2 \end{pmatrix} \qquad (2)$$

$$= 2S_z \otimes \left(A + \delta L_z + dL_z^2\right) + \gamma S_- \otimes L_+ + \bar{\gamma} S_+ \otimes L_-.$$

Let K be the complex conjugation and $\sigma_1 = \sigma_1^{-1} = \begin{pmatrix} 0 & 1 \\ 1 & 0 \end{pmatrix}$,

then if $\delta = 0$

$$(\sigma_1 K) H_{\rm quantum} (\sigma_1 K)^{-1} = -H_{\rm quantum}$$

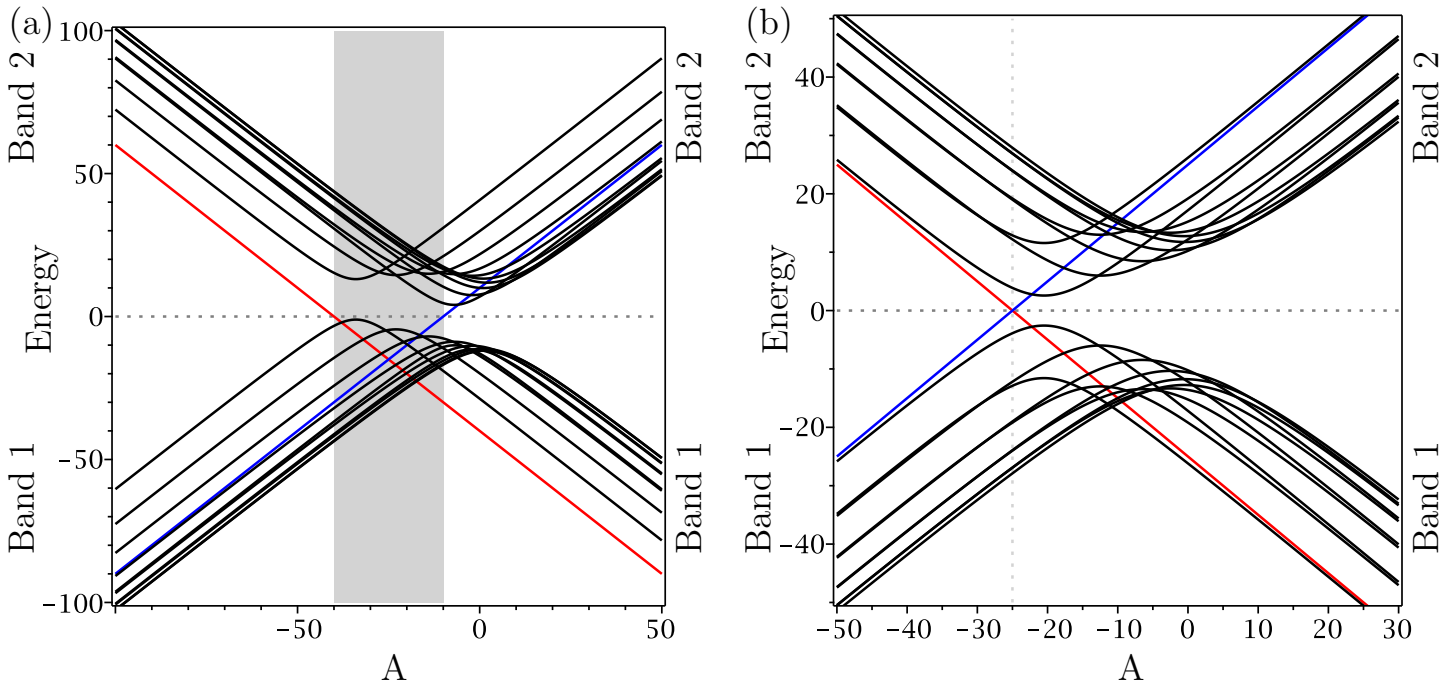

Evolution of the pattern of quantum energy levels of the Hamiltonian (2) under variation of control parameter A. Blue and red lines correspond to two one-dimensional blocks associated with quantum levels going from one band to another. Figures are done for the following choice of phenomenological parameters of the Hamiltonian (2): (a) $L = 5$, $\gamma = 1 + I$, $d = 1$, $\delta = 0$. (b) $L = 5$, $\gamma = 1 + 2I$, $d = 1$, $\delta = -3$.

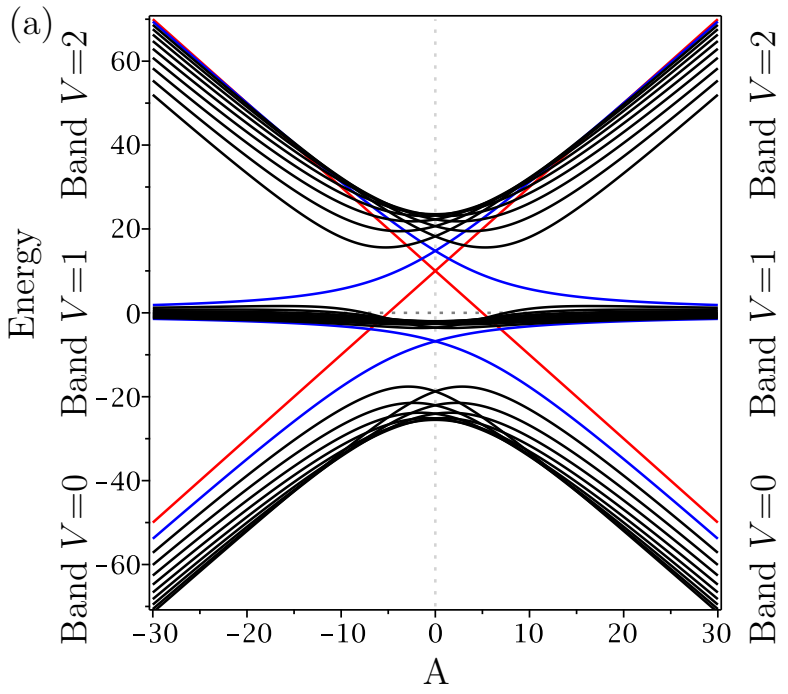

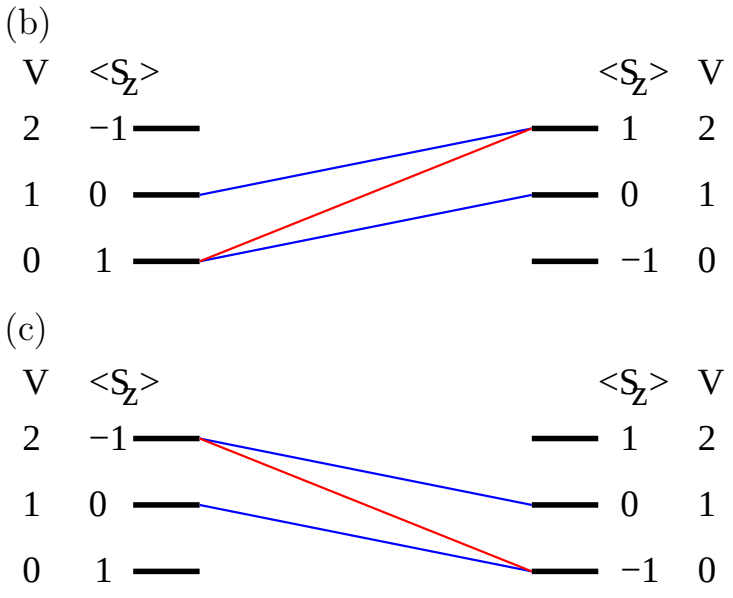

Quantum energy level pattern for $S = 1$ problem. (a) General view of the quantum energy level pattern. (b) Correlation diagram showing the redistribution of energy levels between the $A \to -\infty$ and the $A \to \infty$ limits. Only the levels which change bands under control parameter A variation are shown.

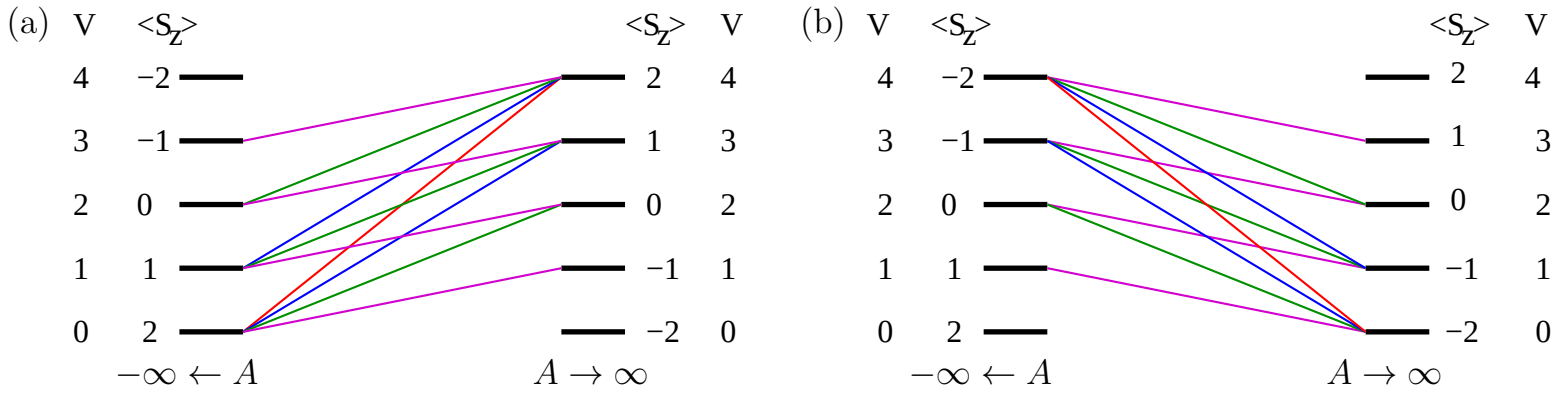

Correlation diagram for $S = 2$. The bands are symbolized by a horizontal thick lines. Only the levels which change bands under control parameter A variation are shown. The levels belonging to invariant subspaces $J_z = -L - S_z$ and $J_z = L + S_z$ ($S_z = S, S-1, ... -S+1$) are shown in separate sub-figures, left and right respectively.

Semi-quantum model

Semi-quantum Hamiltonian with slow variables x_k restricted by $x_1^2 + x_2^2 + x_3^2 = 1$.

$$H_{\mathrm{semi-quantum}} = \begin{pmatrix} A + \delta x_3 + d x_3^2 & \bar{\gamma}(x_1 - i x_2) \\ \gamma(x_1 + i x_2) & -A - \delta x_3 - d x_3^2 \end{pmatrix}, \qquad (3)$$

The two eigenvalues

$$\lambda_\pm = \pm \sqrt{\left(A + \delta x_3 + d x_3^2\right)^2 + |\gamma|^2 \left(x_1^2 + x_2^2\right)}. \qquad (4)$$

Energy reflection symmetry is valid for any δ

$$i\sigma_2 \overline{H_{\mathrm{semi-quantum}}}(-i\sigma_2) = -H_{\mathrm{semi-quantum}} \qquad (5)$$

with $i\sigma_2 = \begin{pmatrix} 0 & 1 \\ -1 & 0 \end{pmatrix}$.

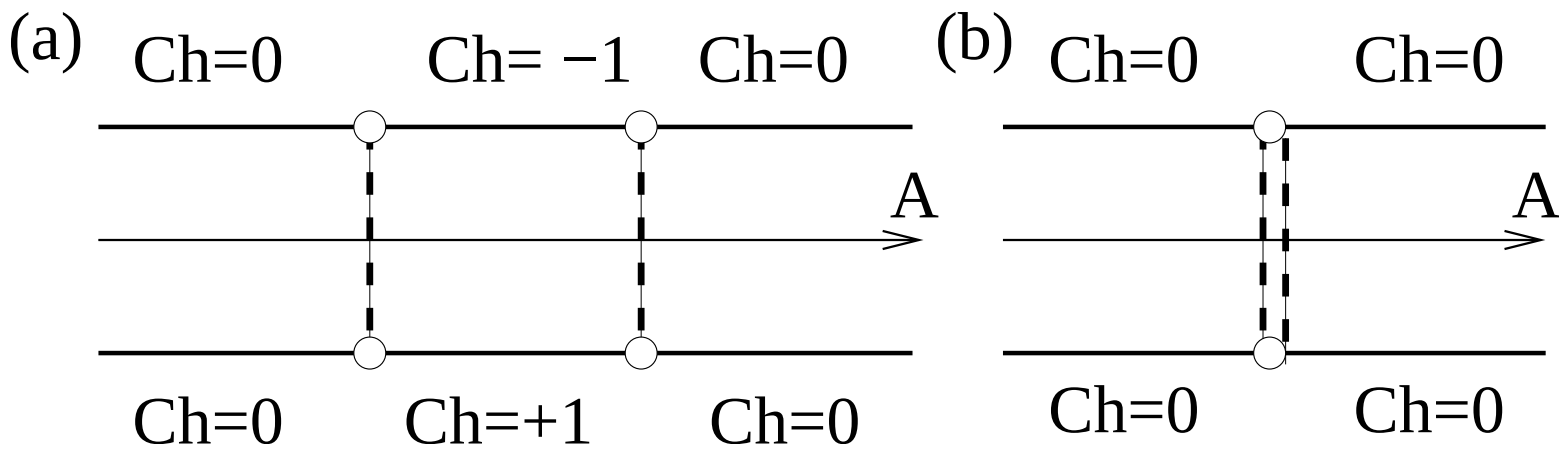

Schematic representation of the evolution of the two eigenline bundles of $H_{\mathrm{semi-quantum}}$ Hamiltonian.

(a) Case of $\delta \geq 0$. (b) Case of $\delta = 0$.

For $\delta \leq 0$ the Chern numbers $\mathrm{Ch} = \pm 1$ should be interchanged.

Completely classical version

Classical Hamiltonian

$$H_{\text{classical}} = 2S_z(A + \delta L_z + dL_z^2) + 2\gamma_r\tau - 2\gamma_i\sigma, \tag{6}$$

with $\tau = S_xL_x + S_yL_y$ and $\sigma = S_xL_y - S_yL_x$ is defined over $S^2 \times S^2$ phase space. On account of SO(2) symmetry the quantity $J_z = L_z + S_z$ is an intergal of motion.

The space of orbits is defined by

$$\tau^2 \leq \left(|\mathbf{S}|^2 - S_z^2\right)\left(|\mathbf{L}|^2 - L_z^2\right). \tag{7}$$

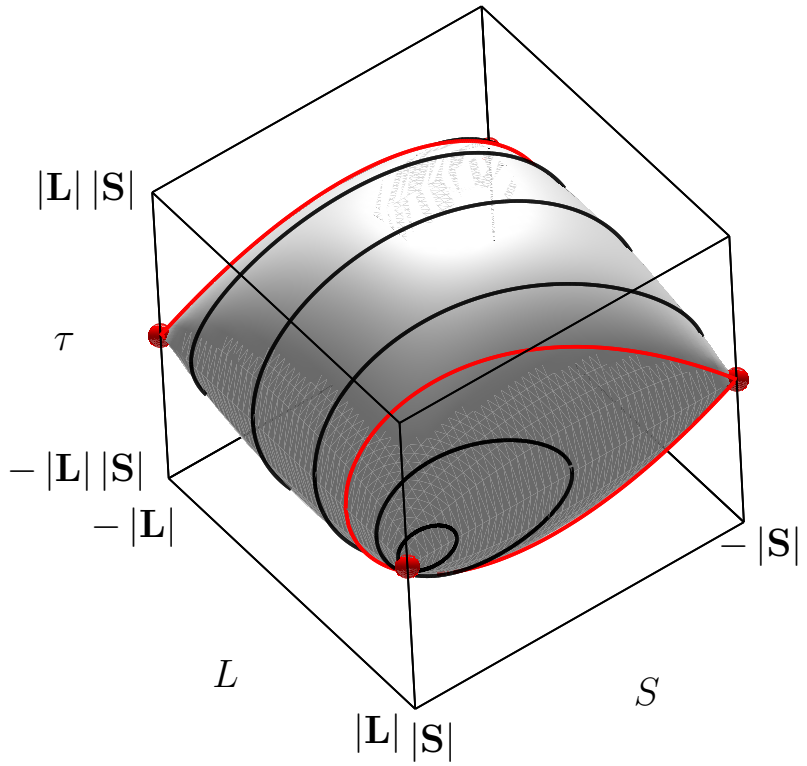

Space of orbits sliced by $J_z = \mathrm{const}$ planes. Black curves: intersection of the space of orbits which contains only regular points. Red curves: intersection of the space of orbits which contains a singular point.

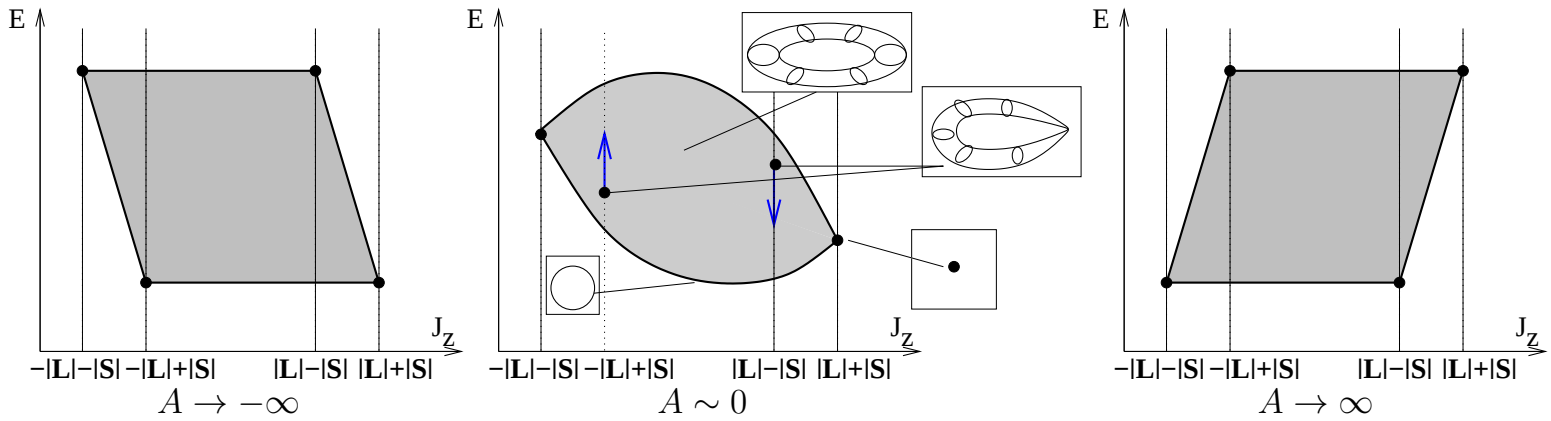

Image of the energy–momentum map for Hamiltonian $H_{\text{classical}}$ (6) with $\delta \approx 0$, $d \approx 0$, $\gamma_i \approx 0$. The blue arrows show the displacement of the critical values with increasing A. (a) Limit $A \to -\infty$. (b) $A \sim 0$. (c) Limit $A \to \infty$.

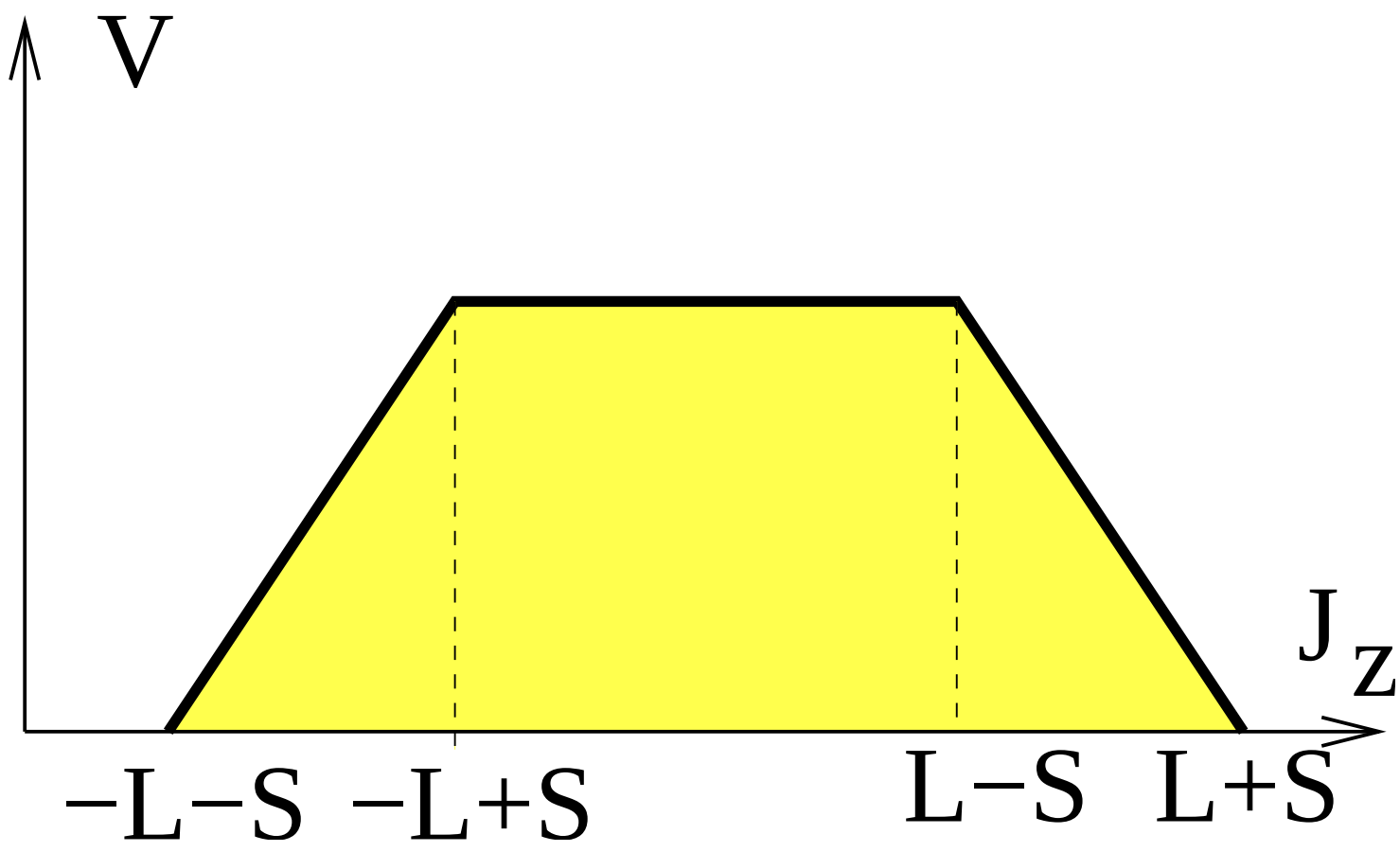

Volume of the reduced phase space V as function of the integral of motion J_z for a classical dynamic system defined over the $S^2 \times S^2$ classical phase space in the presence of axial symmetry.

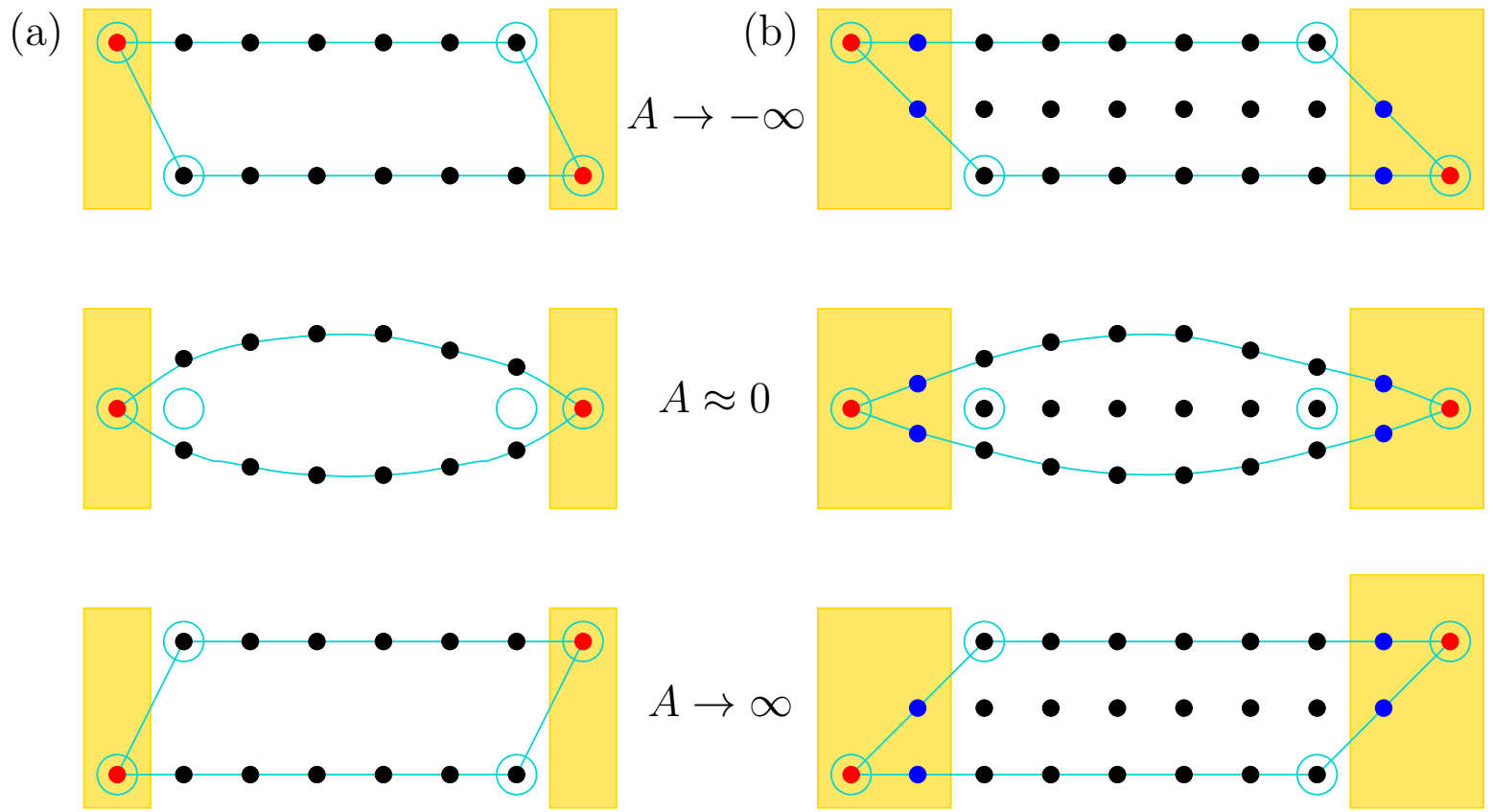

Evolution of the image of the energy–momentum map for Hamiltonian $H_{\text{classical}}$ together with the lattice of quantum states for $S = 1/2$ (left) and $S = 1$ (right). Yellow hatching shows the subset of quantum states redistributing between energy bands under the variation of the control parameter.

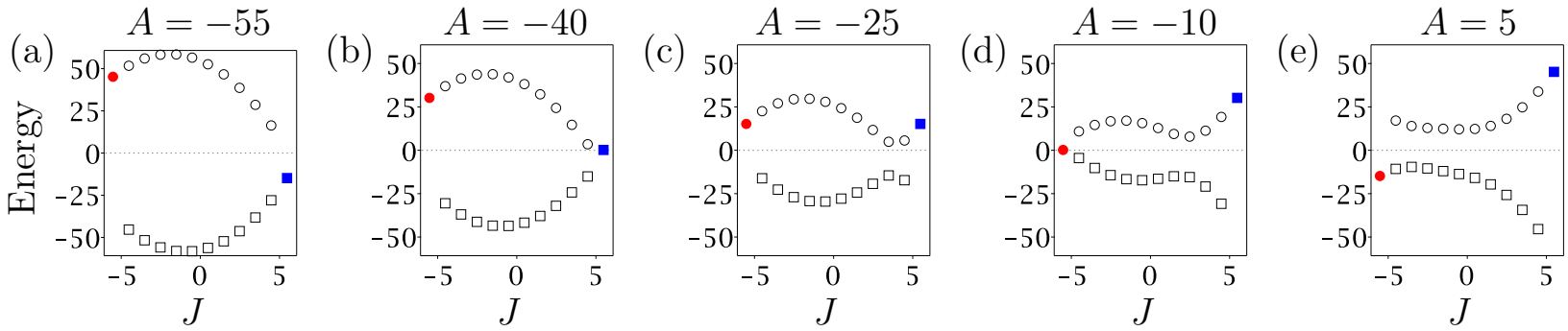

Evolution of the joint spectrum of the Hamiltonian (2) with $L = 5$, $\gamma = 1 + 2i$, $d = 1$, $\delta = 3$. The different subfigures correspond respectively to different A values with $A = -40$ and $A = -10$ cases being associated with “wall-crossing”.

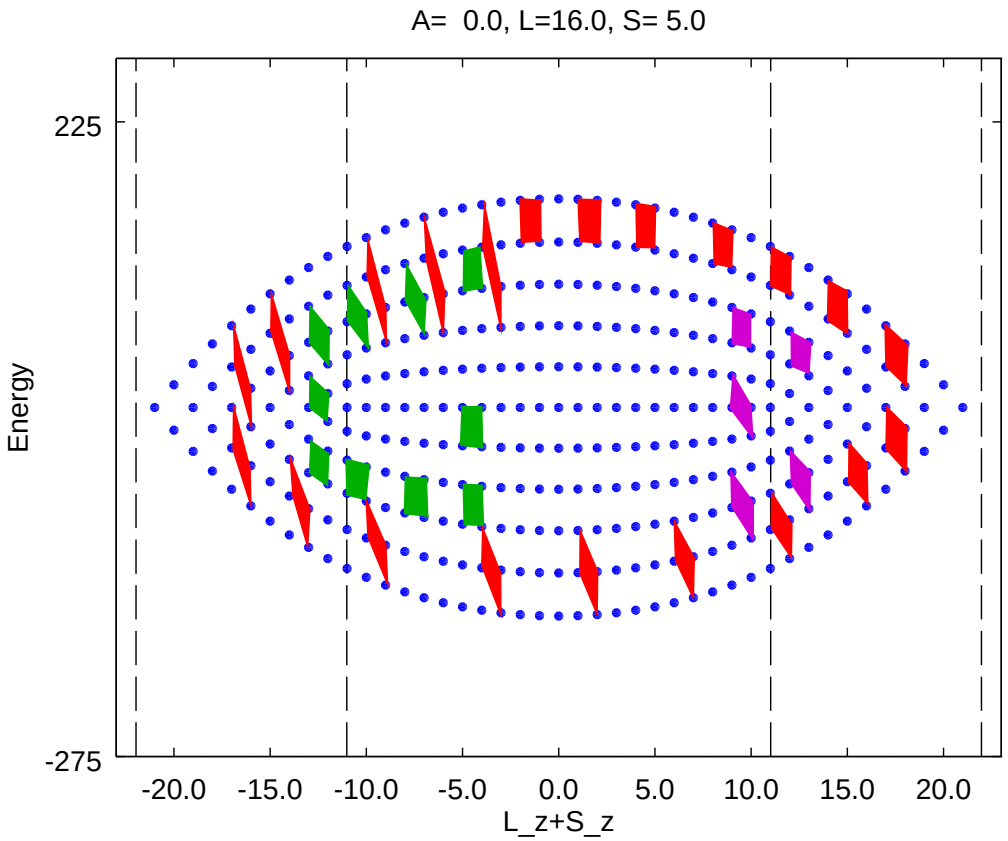

Quantum state lattice for Hamiltonian (2) with $\delta = d = A = 0$, $\gamma = 1$, $L = 16$, $S = 5$. Two elementary monodromy defect of the quantum state lattice become visible by following the evolution of an elementary cell of the lattice along a path surrounding each elementary defect (green and magenta cells).

Semi-quantum models for time-reversal systems with half-integer spin

AII symmetry class = Semi-quantum model for two Kramers doublets

2×2 hyperhermitian quaternionic matrix with zero trace

$$\begin{pmatrix} g & a + b\mathbf{i} + c\mathbf{j} + d\mathbf{k} \\ a - b\mathbf{i} - c\mathbf{j} - d\mathbf{k} & -g \end{pmatrix}; \quad (a, b, c, d, g \in \mathbb{R}). \tag{8}$$

We can always choose trace to be zero by appropriate choice of zero energy.

Quaternions can be represented by matrices:

$$\mathbf{i} = \begin{pmatrix} i & 0 \\ 0 & -i \end{pmatrix} = i\sigma_z; \quad \mathbf{j} = \begin{pmatrix} 0 & 1 \\ -1 & 0 \end{pmatrix} = i\sigma_y; \quad \mathbf{k} = \begin{pmatrix} 0 & i \\ i & 0 \end{pmatrix} = i\sigma_x,$$

where $\sigma_x, \sigma_y, \sigma_z$ are standard Pauli matrices, satisfying the rules

$$\mathbf{i}^2 = \mathbf{j}^2 = \mathbf{k}^2 = \mathbf{ijk} = -1. \tag{9}$$

2×2 quaternionic matrix can be rewritten as 4×4-matrix over real

$$\begin{bmatrix} g & 0 & a+ib & c+id \\ 0 & g & -c+id & a-ib \\ a-ib & -c-id & -g & 0 \\ c-id & a+ib & 0 & -g \end{bmatrix}. \tag{10}$$

with eigenvalues

$$E_{1,2;3,4} = \pm\sqrt{a^2+b^2+c^2+d^2+g^2}. \tag{11}$$

For *semi-quantum model* we consider coefficients a, b, c, d, g as real functions *over classical phase space.*

Codimension of degeneracy of two eigenvalues is 5.

Generic semi-quantum Hamiltonian with four-dimensional classical phase space (base of the fiber bundle) has no degeneracy points.

A one-control-parameter family of semi-quantum Hamiltonians with four-dimensional base space typically has isolated degeneracy points.

Formation of degeneracy points is a
topological phenomenon.

Possible physical examples for “slow“ base space

for two doublet electronic states

- Two vibrational degrees of freedom - $\mathbf{R}^4$.
- Two vibrational polyads formed by three degenerate vibrations - CP^2.
- Vibrational polyads formed by two doubly degenerate vibrations - $S^2 \times S^2$.
- Internal structure of Rydberg shells - $S^2 \times S^2$.

Simple quaternionic semi-quantum Hamiltonian

$$H_{Q_{model}} = \frac{p_1^2 + q_1^2 + p_2^2 + q_2^2}{2}$$

$$+ \begin{pmatrix} G & 0 & q_1 + ip_1 & q_2 + ip_2 \\ 0 & G & -(q_2 + ip_2)^* & (q_1 + ip_1)^* \\ (q_1 + ip_1)^\dagger & -(q_2 + ip_2)^{*\dagger} & -G & 0 \\ (q_2 + ip_2)^\dagger & (q_1 + ip_1)^{*\dagger} & 0 & -G \end{pmatrix}$$

Quantum versions of quaternionic model Hamiltonian

$$H = (a_1^+ a_1 + a_2^+ a_2 + 1) + H_s(a_1, a_2, a_1^+, a_2^+); \tag{12}$$

$$A_{q.1}(a, a^+) = \begin{pmatrix} \alpha_1 a_1 + \alpha_2 a_2 & \beta_1 a_1 + \beta_2 a_2 \\ -\overline{\beta}_1 a_1 - \overline{\beta}_2 a_2 & \overline{\alpha}_1 a_1 + \overline{\alpha}_2 a_2 \end{pmatrix},$$

$$A_{q.3}(a, a^+) = \begin{pmatrix} \alpha_1 a_1 + \alpha_2 a_2 & \beta_1 a_1^+ + \beta_2 a_2^+ \\ -\overline{\beta}_1 a_1^+ - \overline{\beta}_2 a_2^+ & \overline{\alpha}_1 a_1 + \overline{\alpha}_2 a_2 \end{pmatrix},$$

$$\alpha_k, \beta_k \in \mathbb{C}, k = 1, 2.$$

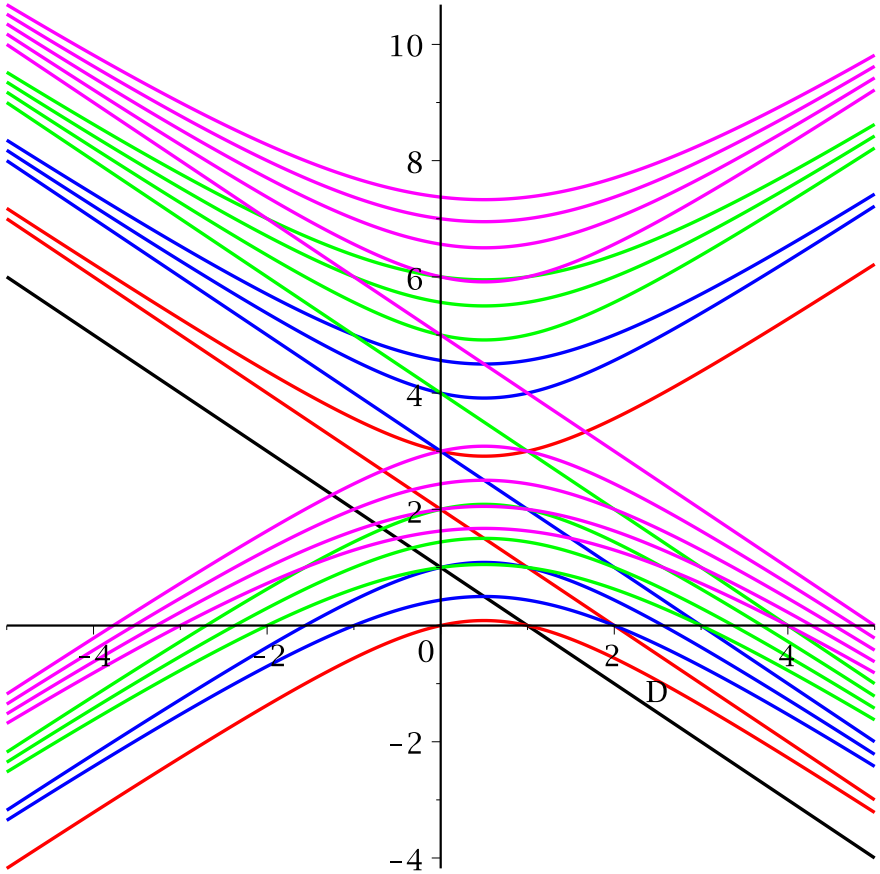

Redistribution of energy levels as a function of control parameter D for Quaternionic model Hamiltonian with finite block structure.

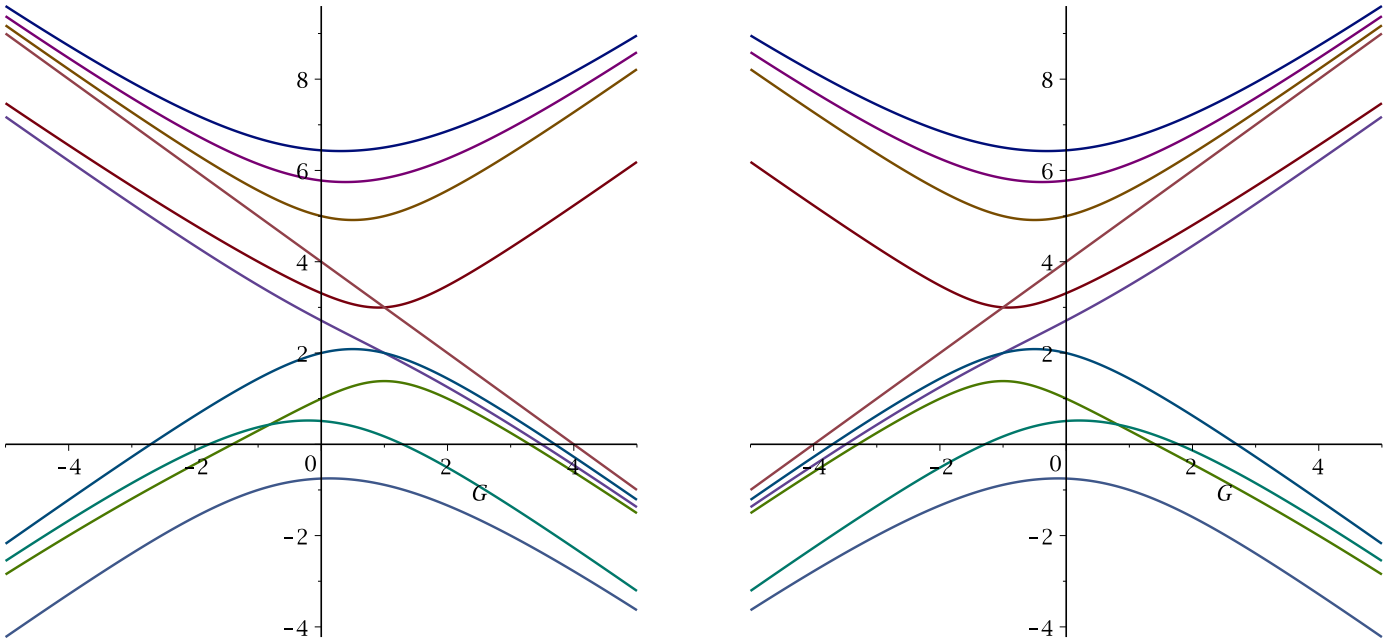

Redistribution of energy levels as a function of control parameter G for Quaternionic model Hamiltonian H_3 with four infinite blocks. Left figure is for A and B blocks possessing degenerate eigenvalues. Right figure is for C and D blocks also having identical eigenvalues. Patterns on the left and on the right figures are related through $G \leftrightarrow -G$ transformation.

Two quantum states with one reality condition

2×2 matrix over S^2 classical phase space after imposing one reality condition $H^* = H$ takes the form (AI symmetry class) :

$$H^{(real)} = \begin{pmatrix} h_{11}(\theta,\phi) & h_{12}(\theta,\phi) \\ h_{12}(\theta,\phi) & -h_{11}(\theta,\phi) \end{pmatrix}, \tag{13}$$

where h_{ij} are real functions. The codimension of degeneracy of two eigenvalues is two. Two conditions should be satisfied

$$h_{11}(\theta,\phi) = 0; \quad h_{12}(\theta,\phi) = 0. \tag{14}$$

Generically, a system of two equations depending on two variables possesses isolated solutions. Small deformation of equations does not change the number of solution but only slightly modifies their position.

Evolution of degeneracy points for one parameter family of real symmetric Hamiltonians.

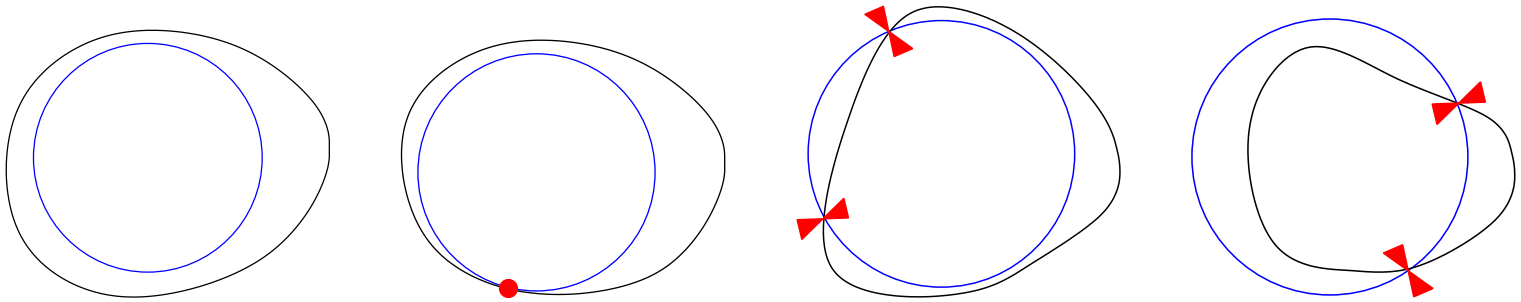

Two curves schematically represent solutions of $h_{11} = 0$ and $h_{12} = 0$ conditions. Intersection of these two curve corresponds to degeneracy point for real symmetric Hamiltonian.

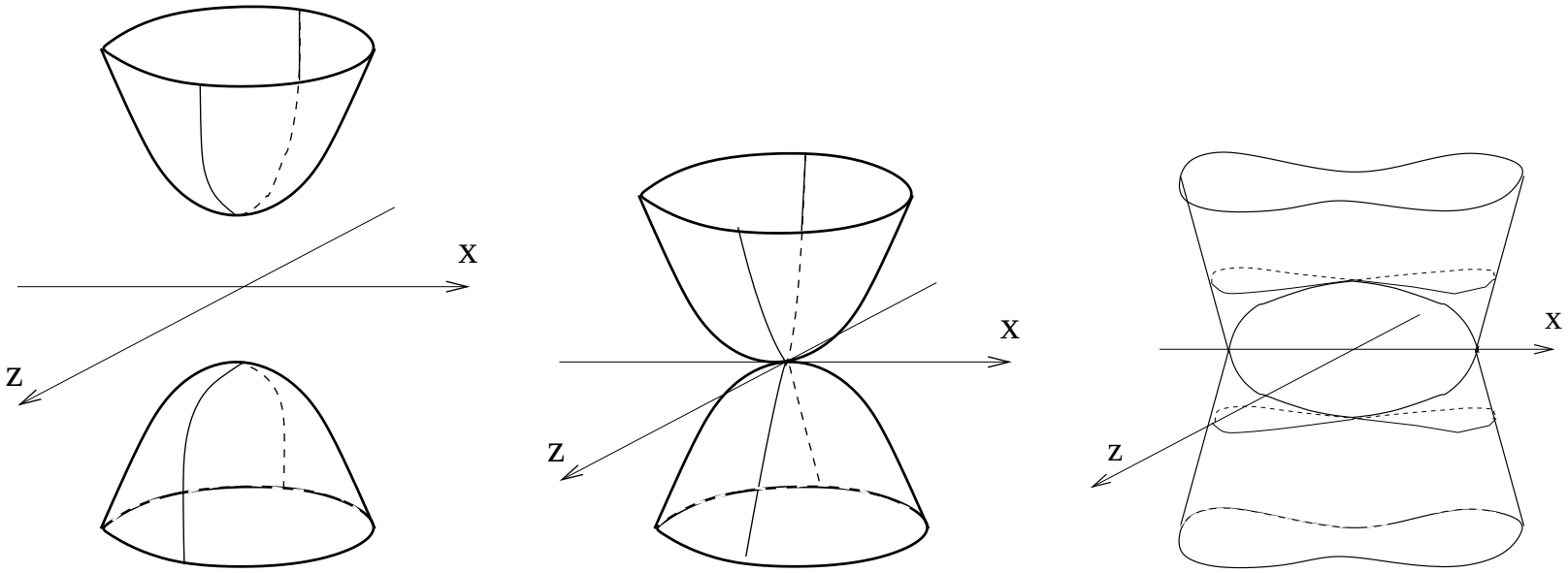

Evolution of two energy surfaces associated with formation of degeneracy points for one parameter family of real symmetric Hamiltonians.

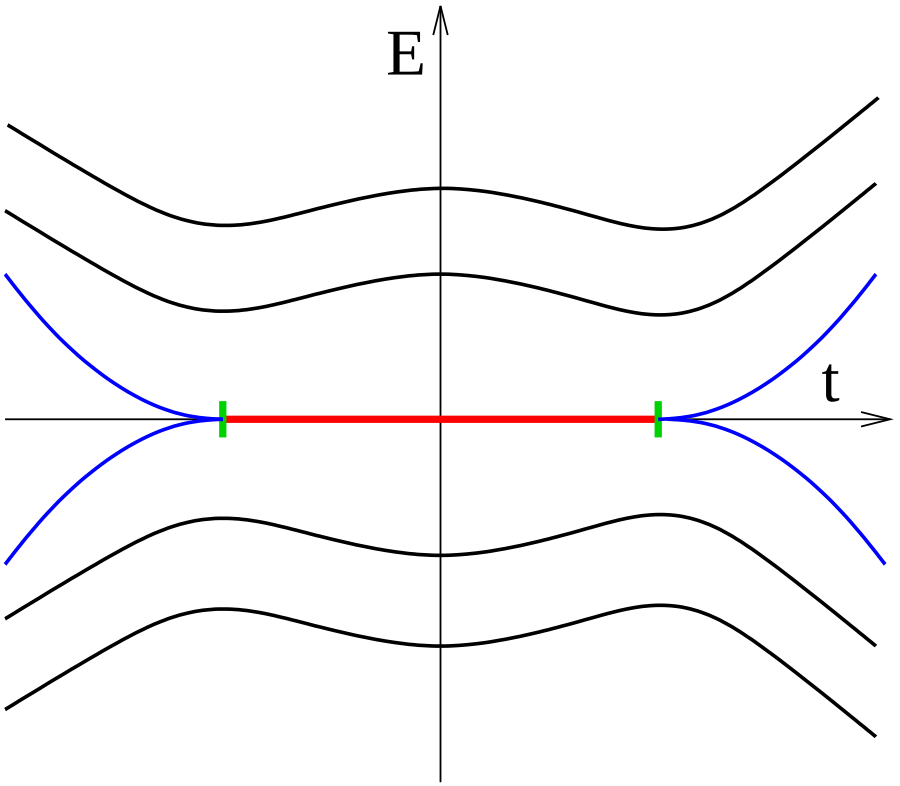

Quantum spectrum of two band semi-quantum model with two degenerate *zero-energy states* which are *robust* under small perturbation respecting the symmetry. Similar energy pattern is discussed for topological insulators, [G.Montamnaux, F. Piechon, J.-N.Fuchs, M.O.Goerbig, Merging of Dirac points in a two-dimensional crystal. Phys.Rev. B80, 153412 (2009), see next slide].

Topological insulators and topological superconductors point of view

A. P. Schnyder, S. Ryu, A. Furusaki, A. W.W. Ludwig, Classification of topological insulators and superconductors in three spatial dimensions. Phys. Rev. B **78**, 195125 (2008).

A. Kitaev, Periodic table for topological insulators and superconductors. Advances In Theoretical Physics: Landau Memorial Conference Chernogolokova (Russia), AIP Conf. Proc. **1134** 22-30 (2009).

B.A. Bernevig, *Topological insulators and topological superconductors.* Princeton Univ. Press, 2013.

Important notions : **“edge states”**

“topologically protected“

“topological phases of matter“

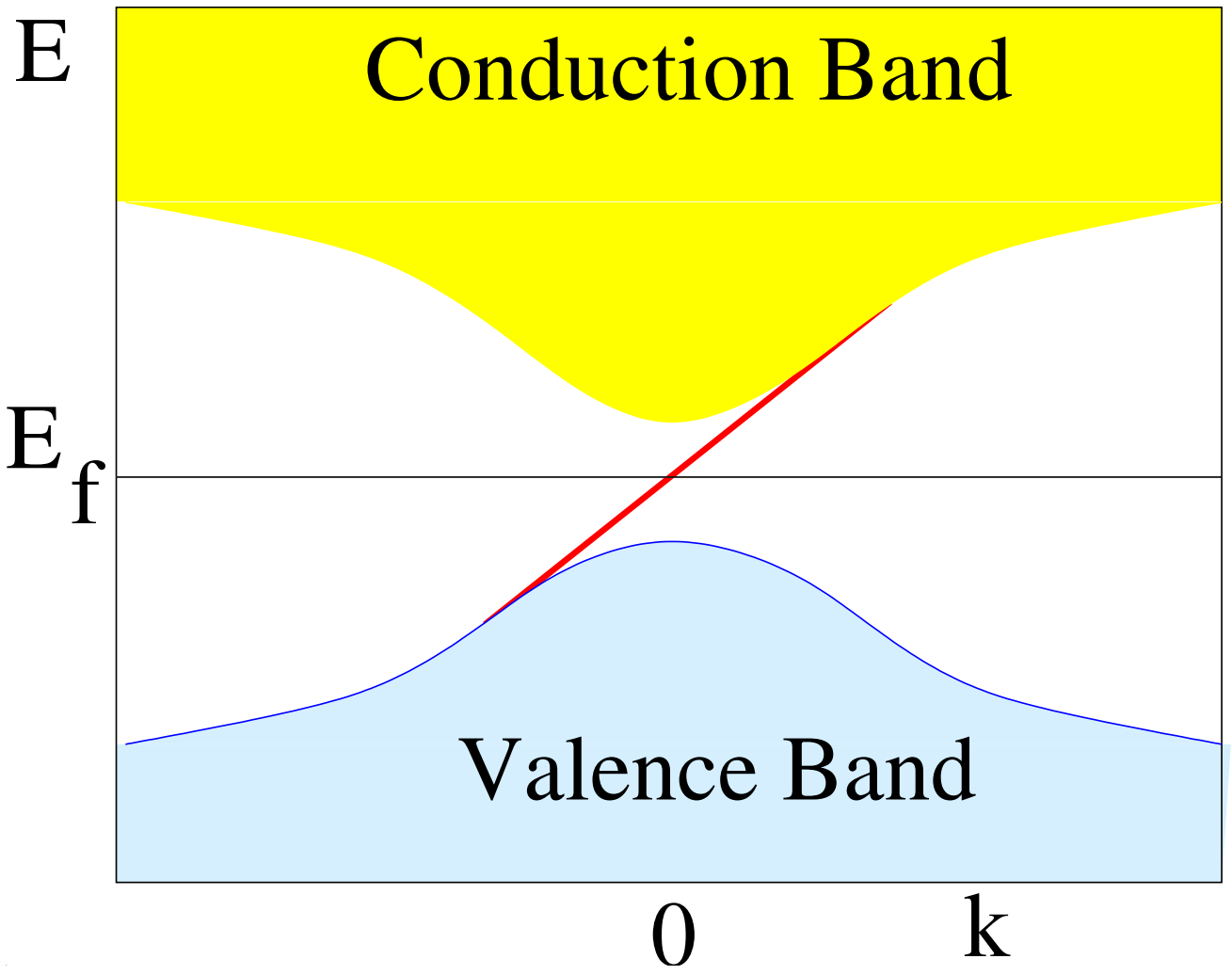

Electronic states for two-dimensional solid as function on the Brillouin cell. [M.Z.Hasan, C.L. Kane, Rev.Mod.Phys. **82**, 3045 (2010).]

Topological insulator classification

There are ten generic symmetry classes of single-particle Hamiltonians.

The Hamiltonians are classified according to their behavior under:

- time-reversal symmetry $\mathcal{T}$,
- charge conjugation (or particle-hole) symmetry $\mathcal{C}$, as well as
- "chiral" (or "sublattice") symmetry $\mathcal{S}$.

$\mathcal{T} H \mathcal{T}^{-1} = H; \quad \mathcal{T}^2 = 1 \quad \text{or} \quad \mathcal{T}^2 = -1; \quad$ (antiunitary operator)

$\mathcal{C} H \mathcal{C}^{-1} = -H; \quad \mathcal{C}^2 = 1 \quad \text{or} \quad \mathcal{C}^2 = -1; \quad$ (antiunitary operator)

$\mathcal{S} = \mathcal{T}\mathcal{C}$; (unitary operator)

Cartan label	$\mathcal{T}$	$\mathcal{C}$	$\mathcal{S}$	Hamiltonian
A (unitary)	0	0	0	U(N)
AI (orthogonal)	$+1$	0	0	U(N)/O(N)
AII (symplectic)	-1	0	0	U($2N$)/Sp($2N$)
AIII (ch. unit.)	0	0	1	U($N+M$)/U(N)$\times$ U(M)
BDI (ch. orth.)	$+1$	$+1$	1	O($N+M$)/O(N)$\times$ O(M)
CII (ch. sympl.)	-1	-1	1	Sp($N+M$)/Sp(N)$\times$ Sp(M)
D (BdG)	0	$+1$	0	SO($2N$)
C (BdG)	0	-1	0	Sp($2N$)
DIII (BdG)	-1	$+1$	1	SO($2N$)/U(N)
CI (BdG)	$+1$	-1	1	Sp($2N$)/U(N)

Topological insulators exibiting merging of Dirac points.

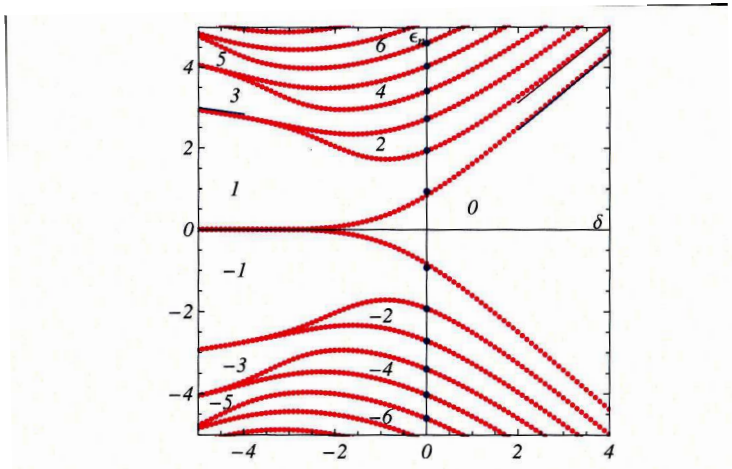

FIG. 3. (Color online) Energy levels $\epsilon_n(\delta)/(m^*c^2\omega^2/2)^{1/3}$ as a function of the dimensionless parameter $\delta \propto \Delta/B^{2/3}$. The dots on the $\delta=0$ axis indicate the semiclassical levels of the quartic Hamiltonian.[4]

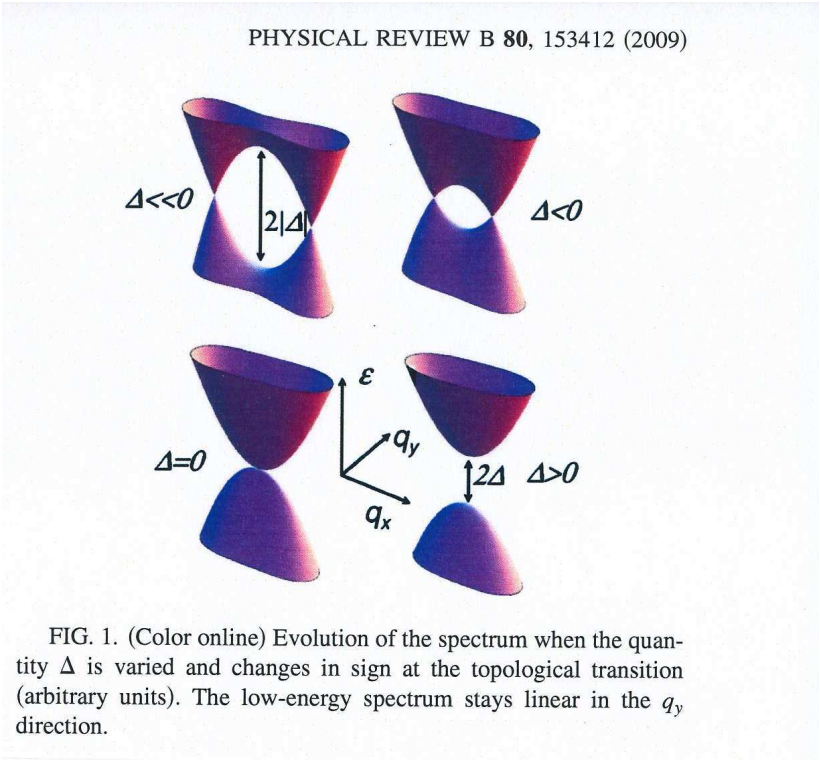

FIG. 1. (Color online) Evolution of the spectrum when the quantity Δ is varied and changes in sign at the topological transition (arbitrary units). The low-energy spectrum stays linear in the q_y direction.

Non-formal analogy between real, complex, quaternionic theories

V.I. Arnol'd. Selecta Math., 1995, **1**, 1-19; In "Mathematics: Frontiers and Perspectives, AMS, 2000

Real	Complex	Quaternionic
$\mathbb{R}$	$\mathbb{C}$	$\mathbb{H}$
$\mathbb{R}P^n$	$\mathbb{C}P^n$	$\mathbb{H}P^n$
$\mathbb{R}P^1 = S^1$	$\mathbb{C}P^1 = S^2$	$\mathbb{H}P^1 = S^4$
Symmetric matrix	Hermitian matrix	Hyperhermitian
O(n)	U(n)	Sp(n)
Codim. of deg.	Codim. of deg.	Codim. of deg.
2	3	5
Stiefel-Whitney	Chern	Pontryagin
Von Neumann-Wigner eigenvalues repulsion	Quantum Hall effect Berry phase	???

Band redistribution for finite particle systems

Comparison of A, AI, AII symmetry classes.

Symm. class	Matrix	Codimension of degeneracy	Characteristic class
AI	symmetric over real	2	Stiefel-Whitney
A	hermitian over complex	3	Chern
AII	hyperhermitian over quaternions	5	Pontryagin (second Chern)